Journal of Colloid and Interface Science 510 (2018) 318–326

Contents lists available at ScienceDirect

Journal of Colloid and Interface Science

journal homepage: www.elsevier.com/locate/jcis

Regular Article

Electrochemical immunoassay for detection of prostate specific antigen based on peptide nanotube-gold nanoparticle-polyaniline immobilized pencil graphite electrode

Tayfun Vural [a], Yesim Tugce Yaman [b], Serhat Ozturk [a], Serdar Abaci [b], Emir Baki Denkbas [a,*]

[a] Biochemistry Division, Department of Chemistry, Hacettepe University, 06800 Ankara, Turkey
[b] Analytical Chemistry Division, Department of Chemistry, Hacettepe University, 06800 Ankara, Turkey

GRAPHICAL ABSTRACT

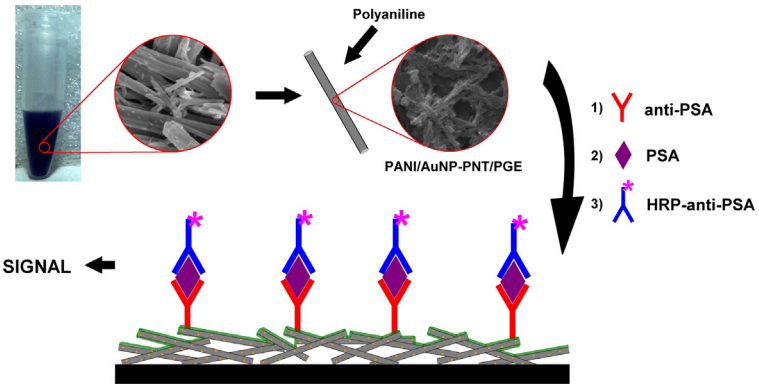

ARTICLE INFO

Article history:
Received 25 June 2017
Revised 19 September 2017
Accepted 21 September 2017
Available online 21 September 2017

Keywords:
Prostate specific antigen
Biosensor
Peptide nanotube
Polyaniline
Gold nanoparticle

ABSTRACT

In this work, we developed a disposable amperometric sandwich-type immunoassay to detect prostate specific antigen (PSA). A self-assembled peptide nanotube (PNT), gold nanoparticle (AuNP) and polyaniline (PANI) composite (PANI/AuNP-PNT) were used to modify a pencil graphite electrode (PGE). Anti-PSA (Ab1) was immobilized on the modified electrode (PANI/AuNP-PNT/PGE) to capture PSA. Horseradish peroxidase (HRP) labeled anti-PSA (HRP-Ab2) was used as a tracer antibody. The modified electrodes were characterized with scanning electron microscopy (SEM), thermogravimetric analysis (TGA), energy dispersive X-ray spectroscopy (EDS), transmission electron microscopy (TEM), cyclic voltammetry (CV), and electrochemical impedance spectroscopy (EIS). PSA concentration in phosphate buffer (pH = 7.4) was determined with electro-catalytic reduction of H_2O_2 on the modified working electrode by using the chronoamperometric method. Limit of detection was found out to be 0.68 ng/mL in a linear range of 1–100 ng/mL with a high regression (R^2 = 0.990). To show the practicality of the modified biosensor in real matrixes, it was successfully applied for the detection of PSA in blood serum samples. The proposed method was also compared with enzyme-linked immunosorbent assay (ELISA) and compatible results were obtained. The developed immunoassay exhibited good reproducibility together with high stability and provides an efficient approach to detect PSA cost-effectively compared to traditional methods.

* Corresponding author.
E-mail addresses: tvural@hacettepe.edu.tr (T. Vural), tugce.yaman@hacettepe.edu.tr (Y.T. Yaman), serhat.ozturk@hacettepe.edu.tr (S. Ozturk), sabaci@hacettepe.edu.tr (S. Abaci), denkbas@hacettepe.edu.tr (E.B. Denkbas).

https://doi.org/10.1016/j.jcis.2017.09.079
0021-9797/

1. Introduction

Prostate specific antigen (PSA) is a type of glycoprotein and is produced by the prostate. PSA is used as a biomarker for the diagnosis of prostate cancer [1,2]. The main function of the PSA enzyme is to break down the gel-forming proteins such as semenogelins I and II in the semen, thereby increasing the motility and productivity of the semen [3]. Though a certain level of PSA is found in the blood serum of a healthy person, this amount is increased in patients. Additionally, it was determined that there was a relationship between the amount of PSA and the level of the disease. PSA level is below 4 ng/mL in healthy men, while it is above 4 ng/mL in prostate cancer patients this level may increase depending on the level of cancer progression [4]. Therefore, the role of PSA plays a pioneering role in prostate cancer. Hence, the rapid, sensitive and alternative methods for the detection of PSA maintains its importance.

In the literature, some conventional methods were usually practiced for the detection of PSA such as enzyme-linked immunosorbent assay (ELISA), radioimmunoassay (RIA), chemiluminescence immunoassay (CLIA), electro-chemiluminescence immunoassay (ECLIA), chemiluminescent microparticle immunoassay (CMIA), fluoro-immunoassay (FIA). Though these procedures are very efficient and highly accurate, the realization of these tests is laborious, time-consuming and quite costly. Therefore, biosensors which work with different principles have been developed to detect biomarkers for enabling early detection of cancer [5–7]. Among these, electrochemical biosensors stand out due to some of their superior features such as rapid and high sensitivity detection, easier, and faster and cheaper monitoring of disease progression [8–10].

Diphenylalanine (FF) dipeptide can form a peptide nanotube (PNT) structure by self-assembly under certain conditions [11,12]. PNTs are promising materials due to their stability, ease of synthesis and biocompatibility [13–16]. Diphenylalanine based peptide nanostructures have attractive properties for many nanotechnological applications such as molecular recognition, drug release, photovoltaic cell, and energy storage [17,18]. Furthermore, the electrical conductivity of PNTs have been studied [19,20] and they have been applied in the electrochemistry field owing to their ease of synthesis and modification, ability to increase the signal/noise ratio, biocompatibility, and stability [21–24]. When PNTs are combined with other sensor materials, they can show a synergistic effect with a high selectivity and sensitivity. For instance, the greatest success of the gold nanoparticles (AuNPs) is to increase the electro-active surface area in catalytic applications [25]. Furthermore, it provides direct electron transfer, has high surface area/volume ratio and shows biocompatible properties [26]. Thus, it is used extensively in biosensor applications in the literature [27]. Conducting polymers like polyaniline (PANI), polypyrrole, poly(o-toluidine), and their composites have been extensively studied in the literature [28–32]. Especially, PANI is a highly remarkable and intensive research topic among conducting polymers. This is due to the fact that polyaniline and its derivatives, composites or co-polymers can be easily synthesized chemically or electrochemically by oxidative polymerization. Thus, PANI has been combined with various nanomaterials and nanoparticles, for improving physicochemical properties of the materials and for the construction of effective detection sensor platforms [33–39]. Considering the studies in the literature, PANI/AuNP-PNT modified sensor application was not found.

Herein, we fabricated PANI/AuNP-PNT modified PGE which was a disposable, cheap, and easy method for the chronoamperometric detection of PSA for the first time. PANI/AuNP-PNT composite enhanced the signal of PSA remarkably due to their synergistic effect, high surface area, and signal/noise ratio. Electrochemical and spectroscopic methods were carried out for revealing the effect of the modification on the electrode surface. ELISA was used as a control method and similar results were obtained with both analysis. We obtained comparable data with similar studies in the previous literature. The developed method demonstrated the adaptability of PSA detection in clinical applications instead of conventional, high cost and time-consuming process.

2. Experimental

2.1. Chemicals and reagents

Gold(III) chloride trihydrate ($HAuCl_4 \cdot 3H_2O$), 1-ethyl-3-(3-dimethylaminopropyl) carbodiimide (EDC), *n*-hydroxysuccinimide (NHS), Bovine serum albumin (BSA), hydroquinone (HQ), phosphate buffer saline (PBS) tablet (pH: 7.4, 10 mM), and aniline were purchased from Sigma-Aldrich. Pencil graphite electrode (PGE, 0.5 mm, HB) was obtained from local market (Tombow Pencil Co. Ltd., Japan). Diphenylalanine was obtained from Bachem, Switzerland. PSA antigen (Ag), anti-PSA antibody (Ab1), and secondary anti-PSA antibody (Ab2) labeled with horseradish peroxidase (HRP) were purchased from Fitzgerald, U.S.A. All aqueous solutions were prepared with Milli-Q deionized pure water with a resistivity of 18.2 MΩ cm. All reagents were analytical grade and used without further purification.

2.2. Instrumentation and measurements

To enlighten the features of the developed electrodes, scanning electron microscopy (SEM, Zeiss Evo 60), thermogravimetric analysis (TGA, Thermo Scientific), energy dispersive X-ray spectroscopy (EDS, Bruker AXS Quantax 4010), transmission electron microscopy (TEM, JEM-1400Plus) were used. All electrochemical measurements were carried out using CH Instrument Potentiostat/Galvanostat in a three-electrode configuration. The modified electrode was used as the working electrode by dipping 1 cm of the electrode in a three-electrode cell. The reference electrode was Ag/AgCl (3.0 M KCl) and the counter electrode was platinum wire. Before measurements, all solutions were deaerated with pure nitrogen gas for about 20 min.

2.3. Fabrication of the biosensor

We synthesized gold nanoparticle/peptide nanotube hybrid nanomaterial to modify pencil graphite electrodes. Firstly, 6.0 mg diphenylalanine was dissolved in 100 μL hexafluoroisopropanol and added in 0.5 mg/mL Gold(III) chloride trihydrate ($HAuCl_4 \cdot 3H_2O$) solution in different concentrations. Then, the solution was sonicated for 10 min and then incubated at 60 °C for an hour. At the end of this period, diphenylalanine self-assembled to form nanotubes and gold nanoparticles was formed. To fabricate AuNP-PNT/PGE, pencil graphite electrode was modified by dipping into AuNP-PNT dispersion and incubated for 5, 15, and 30 min at room temperature. Afterwards, the AuNP-PNT adsorbed electrode was dried and washed with DI water. PANI thin film was synthesized electrochemically onto AuNP-PNT/PGE by cyclic voltammetry. Electro-polymerization of aniline was carried out in an electrolyte solution composed of 0.5 M H_2SO_4 and 1 mM aniline. Cyclic voltammograms (CVs) were recorded at a scan rate of 0.1 Vs^{-1} for a potential range of −0.1 to +1.1 V (vs.Ag/AgCl). Anti-PSA (Ab1) was attached to PANI/AuNP-PNT/PGE surface via 1-Ethyl-3-(3-dimethylaminopropyl) carbodiimide (EDC)/*n*-hydroxysuccinimide (NHS) amidization reaction described by Arya et al. [40]. To activate COOH group of Ab1, a solution was prepared containing 0.4 M EDC, 0.1 M NHS, and 10 μg/mL Ab1 in

PBS solution (pH: 7.4, 10 mM). To obtain amide bonds between the COOH group of Ab1 and the NH_2 group of PANI, PANI/AuNP-PNT/PGE was dipped into the solution and incubated for 2 h at room temperature. To remove any unbound Ab1, electrodes were washed with 0.05% Tween-20 in PBS solution and PBS solution subsequently. Preventing nonspecific binding of Ab1 is essential to obtain good sensitivity for biosensor. Then, Ab1 modified electrodes were incubated for an hour with 2% BSA at room temperature and then washed with 0.05% Tween-20 in PBS solution and PBS solution subsequently. Later electrodes were incubated with PSA (Ag) in PBS solution (0–100 ng/mL) at different durations (15, 30 and 60 min), followed by washing with 0.05% Tween-20 in PBS solution and PBS solution. Then, the electrodes modified with PSA were finally incubated with HRP labeled secondary antibodies (Ab2) for an hour at room temperature. And the final modified electrodes were washed with 0.05% Tween-20 in PBS solution and PBS solution before using them in electrochemical analyses [41].

3. Results and discussion

3.1. Characterization of the modified electrodes

Fig. 1 showed the surface morphology of PANI/AuNP-PNT/PGE and PGE obtained with scanning electron microscope. According to Fig. 1A and B, PANI and AuNP-PNT structures were adsorbed on PGE. Also, PANI film, occurring due to successful synthesis from aniline by cyclic voltammetry, was observed on AuNP-PNT. Compared to the smooth, bitty and disorderly layered surface of PGE, PANI/AuNP-PNT/PGE had PANI film coated PNT structures were observed on the surface of the PANI/AuNP-PNT/PGE.To determine the elemental composition of PANI/AuNP-PNT/PGE, energy dispersive X-ray spectroscopy (EDS) was performed (Fig. 2). EDS spectrum shows the presence of carbon (C) and nitrogen (N) which present in PANI and PNT. Oxygen (O) is also present in the structure of the PNT. Two characteristic X-ray energy peaks of gold (Au) in the spectrum proved that composite includes gold nanoparticles. Consequently, the EDS spectrum confirms the successful modification of PGE with AuNP-PNT and PANI.

The increase in the electroactive surface area of the PANI/PGE, PANI/PNT/PGE, and PANI/AuNP-PNT/PGE was determined by CV (Fig. S1) in 5 mM $Fe(CN)_6^{4-/3-}$ solution containing 0.1 M KCl according to the Randles–Sevcik Eq. (1)

$$I_{pa} = 2.69 \times 10^5 A \times D^{1/2} n^{3/2} v^{1/2} C \quad (1)$$

where I_{pa} is anodic peak current. A refers electroactive surface area. D, n, and v show the diffusion coefficient, the number of transferred electrons, and scan rate, respectively. C shows the concentration of the redox probe ferri- and ferrocyanide. Modification of PGE with PANI and PANI/PNT increased electroactive surface area about 5.3% and 10.5%, respectively. As a result of modification with PANI/AuNP-PNT, the effective surface area of the electrode increased about 18.6%.

Electrochemical impedance spectroscopy (EIS) was used to investigate the modification of electrodes at each step. Fig. 3 shows overlapped impedance spectra as a nyquist plot of electrodes in a solution containing 5 mM $Fe(CN)_6^{3-/4-}$ and 0.1 M KCl.

Nyquist plots were obtained in a frequency range of $10–10^5$ Hz with an amplitude of 25 mV. It is clear that adsorption of AuNP-PNT on PGE decreased the charge transfer resistance (R_{CT}) of the electrode. The spatially aligned aromatic structure of the peptide nanotube caused faster electron transfer rate and contributed to conductivity and electro-activity [18]. Filho et al. calculated band gaps of peptide nanotubes and found comparable results with the inorganic nanotubes. They also showed that interaction of water molecules with PNT increases the dipole moment, the hopping electron probabilities and consequently the conductivity of the PNT [42]. Overall, we can say that peptide nanotubes promoted electron transfer on the electrode. AuNP is known as a good electrical conductive nano-sized material which increases electroactivity. When AuNP-PNT/PGE was modified with PANI, R_{CT} decreased again. This shows us that the conductive polymer PANI was synthesized successfully by electro-polymerization of aniline on the electrode surface. Next Ab1, BSA, Ag, and Ab2 modifications of PANI/AuNP-PNT/PGE were carried out and each modification step showed an increase in the R_{CT} value of the electrode in accordance with the literature [43]. It can be proposed that the reason for the decrease in R_{CT} value is due to the blocking of electron transfer by biomolecules on the modified electrode surface.

The electron transfer rate constant (k_s) and the charge transfer coefficient (α) for the HRP/Ab2/Ag/Ab1/PANI/AuNP-PNT/PGE was calculated with Laviron equation by using cyclic voltammetry [44,45]. According to Fig. S2, the anodic peak potential (E_{pa}) and the cathodic peak potential (E_{pc}) have a linear relationship with the logarithm of scan rates. The charge transfer coefficient can be calculated from the slopes of the plots using the following equation:

$$k_a \,/\, k_c = \alpha/\,(1-\alpha) \quad (2)$$

where k_a and k_c are the slope of the plots for E_{pa} versus logv and E_{pc} versus logv, respectively. Thus, the value of α was calculated to be 0.65. In addition, the electron transfer rate constant can be also calculated using the following equation:

$$log\ k_s = \alpha log(1-\alpha) + (1-\alpha) log\alpha - logRT/nFv - \alpha(1-\alpha)nF\Delta E_p/2.3RT \quad (3)$$

where n is the number of electrons transferred, ΔE_p is the peak-to-peak potential separation, v is the scan rate, and other symbols

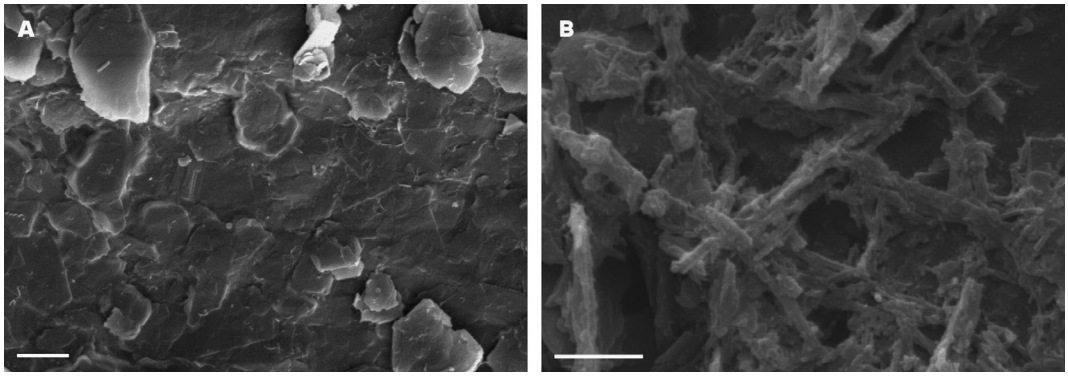

Fig. 1. SEM images of bare pencil graphite electrode (A) and PANI/AuNP-PNT modified pencil graphite electrode (B). The scale bars represent 2 μm.

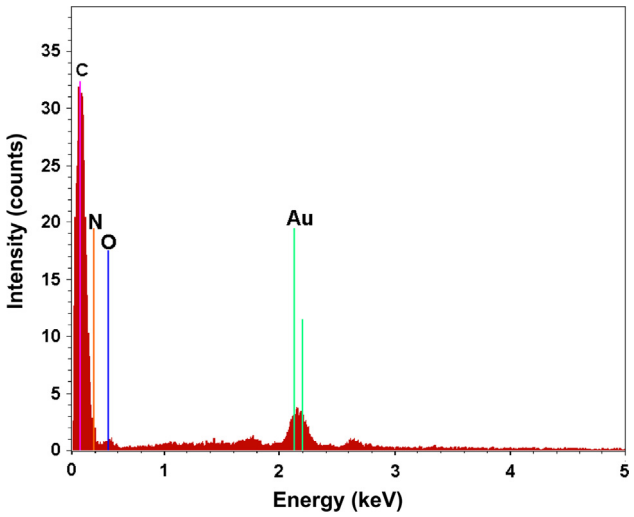

Fig. 2. EDS spectrum of PANI/AuNP-PNT/PGE.

have their usual meanings. The calculated value for k_s was 2.3×10^{-3} s^{-1} at 100 mV s^{-1}.

After the characterization step of the biosensor, it was planned to use the developed surface for the sensitive detection of PSA. Before detection, various parameters which might affect the biosensor response were investigated and optimized. These parameters and results are given as follows.

3.2. Optimization of parameters that affected the biosensor response of surface

3.2.1. Effect of $HAuCl_4$ concentration on PNT formation

Reduction of Au (III) ions and growth mechanism of gold nanoparticles has been reported in the literature previously [45]. According to author, Au (III) ions are converted into metallic Au (0) by a reducing reagent and then AuNPs are formed via nucleation and growth of single crystals [46]. Also, peptide nanotube formation from diphenylalanine is well-known self-assembly process. The hydrophobic interactions, π-π stacking, and hydrogen bonds play a major role in self-assembly of nanotubular peptide structure [47,48]. Besides, peptides have the ability to reduce $AuCl_4^-$ and to form gold nanoparticles through the amino and carbonyl groups [49]. In the light of these informations, we think that the reduction of gold nanoparticles results in oxidation of peptide nanotubes.

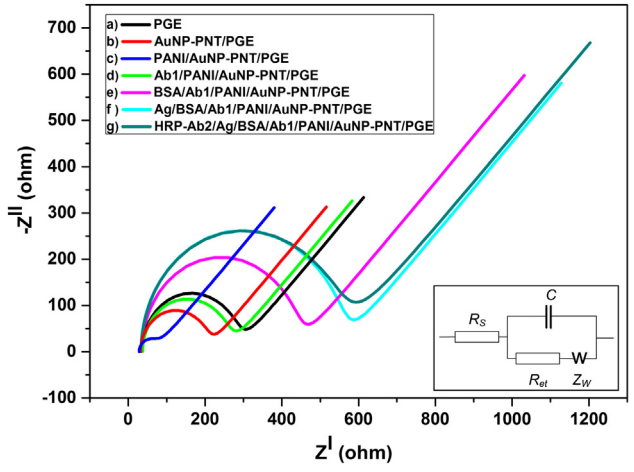

Fig. 3. Nyquist plots for pencil graphite electrodes at each modification step in 0.1 M KCl solution containing 5 mM $[Fe(CN)_6]^{4-/3-}$. The inset shows the equivalent circuit for the impedance spectra.

The solutions formed by adding the diphenylalanine solution to the $HAuCl_4$ at different concentrations were shown in Fig. 4A. When diphenylalanine concentration reached at 6.0 mg/mL in aqueous solution, dipeptides formed nanotubes due to intermolecular forces [50]. In order to construct AuNP-PNT composite, different concentrations of $HAuCl_4$ solution added to the solution. It was determined that solutions containing $HAuCl_4$ at 0.1 and 0.5 mg/mL concentrations contained both AuNP and PNT structures. But, the solutions containing $HAuCl_4$ at 2.0 mg/mL and 5.0 mg/mL did not form PNT structures. Additionally, there was a color change in dispersions with the change of $HAuCl_4$ concentration. The color of dispersions for 0.1 and 0.5 mg/mL $HAuCl_4$ was light violet and navy blue, respectively. When we used 2.0 and 5.0 mg/mL $HAuCl_4$, brown precipitations appeared as can be seen in Fig. 4A. The observations we present here suggest that when we use a high concentration of $AuCl_4^-$, intermolecular interactions are affected and nanotubular structure is distributed and caused to the formation of distinct oxidized aggregated peptides.[1]

The solution containing 0.5 mg/mL $HAuCl_4$ was used for electrode modification because it contained peptide nanotube structures as suspension with higher gold nanoparticle content. The structures formed by self-assembly diphenylalanine in the aqueous solution of $HAuCl_4$ was also investigated by scanning electron microscopy (SEM) (Fig. 4B). As seen from Fig. 4B.b, this formulation promoted the formation of PNT and it preserved the nano-tubular structure. Also, this construction contained the high incidence of AuNP. Thus, modification of PGE was carried out using 0.5 mg/mL $HAuCl_4$ and 6.0 mg/mL diphenylalanine.

The AuNP-PNT composite was also investigated by transmission electron microscopy (TEM). Fig. 5 clearly demonstrated that the AuNPs and the PNTs were synthesized successfully as a nanocomposite and the AuNPs were formed into interlayer space. The AuNPs were found to be in non-uniform shape and predominantly in the size range of 20–50 nm. Also, PNTs had a diameter range of 300–800 nm.

Thermogravimetric analysis was carried out to determine the amount of AuNP in AuNP-PNT nanocomposite (Fig. S3). Obtained AuNP-PNT was heated from room temperature to 500 °C in a N_2 atmosphere. The decrease in the weight of the composite around 300 °C resulted from the degradation of PNT. After that temperature weight reached a low plateau at around 320 °C and no negligible weight loss was observed. The noncombustible AuNP were left as a residue at 500 °C with an amount of 7.1%.

3.2.2. Effect of AuNP-PNT adsorption time

PGE electrodes were kept in an AuNP-PNT solution with different durations to optimize adsorption time of AuNP-PNT onto PGE. For this purpose, PGEs were immersed into 1 ml AuNP-PNT solution at 5, 15, 30 min respectively. After this step, electropolymerization of aniline was carried out by cyclic voltammetry (5 cycles were run between the – 0.1 to 1.1 V (vs.Ag/AgCl). PANI/AuNP-PNT/PGE electrodes were inserted into 5 mM $K_3[Fe(CN)_6]$/$K_4[Fe(CN)_6]$ solution to determine the electrochemical activity by cyclic voltammetry. The obtained cyclic voltammograms of PANI/AuNP-PNT/PGE was shown in Fig. 6. It was found that maximum current density was obtained at for 15 min adsorption time. After that time, the response did not significantly change due to reaching saturation. Thereby, the optimum physical adsorption time of AuNP-PNT was determined as 15 min.

[1] For interpretation of color in Fig. 4, the reader is referred to the web version of this article.

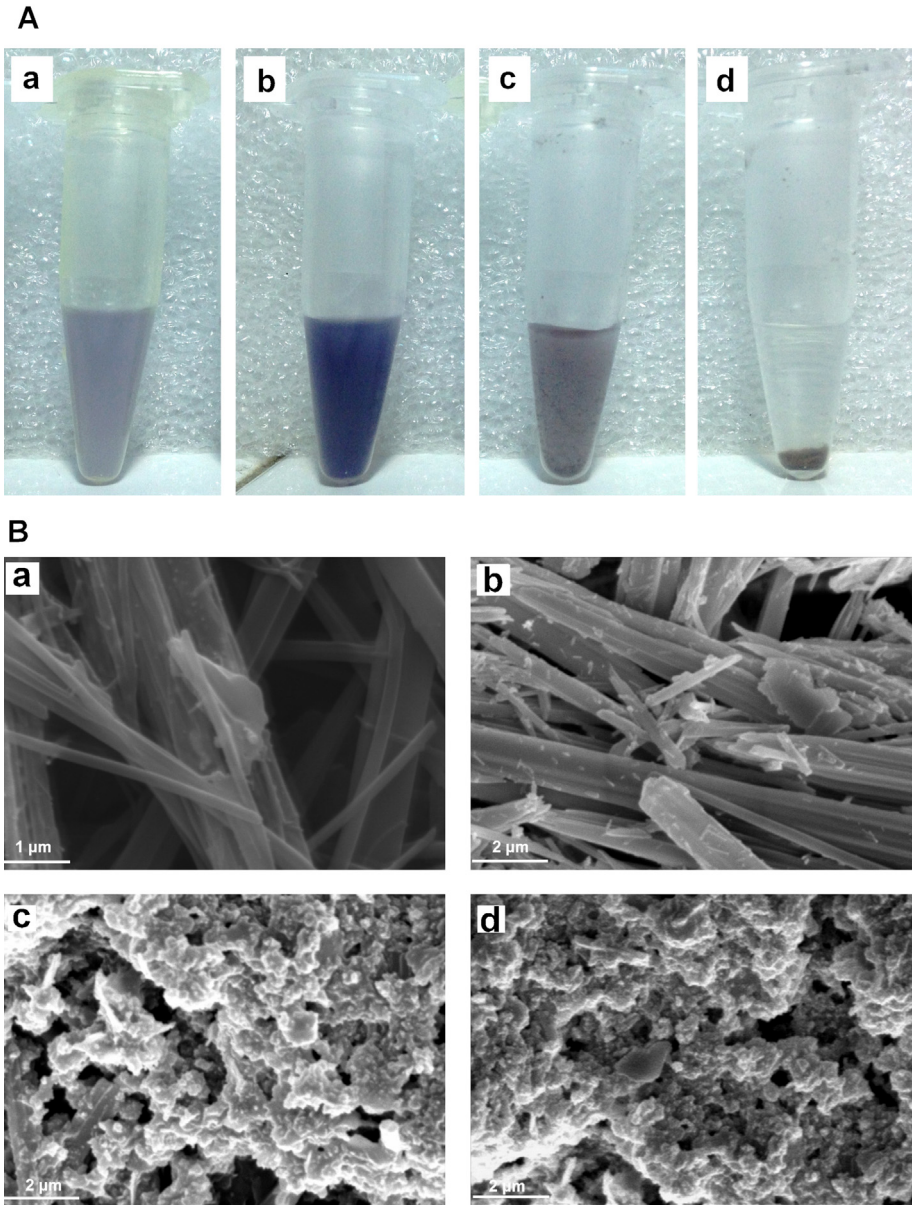

Fig. 4. (A) The effect of the concentration of $HAuCl_4$ on the formation of AuNP-PNT composite, (B) SEM images of AuNP-PNT composite obtained with different concentration of $HAuCl_4$ (a) 0.1 mg/mL, (b) 0.5 mg/mL, (c) 2.0 mg/mL and (d) 5.0 mg/mL.

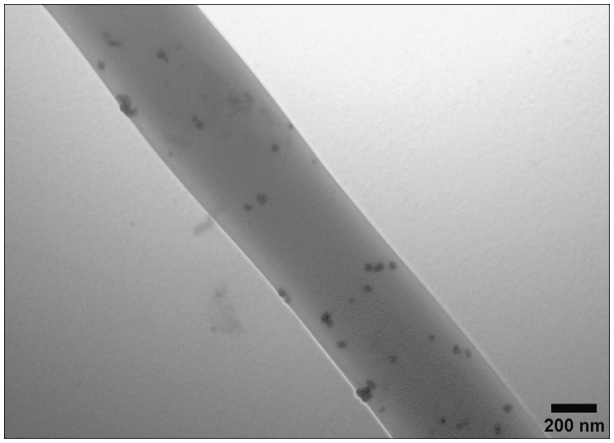

Fig. 5. TEM image of AuNP-PNT nanocomposite.

3.2.3. Effect of polymer thicknesses

Polyaniline is synthesized by polymerization of aniline and can exist in three different oxidation states: Emeraldine (E), Leucoemeraldine (L), and Pernigraniline (P). The fully reduced transparent form is L, fully oxidized blue form is P, and half-oxidized green form is E which is the only conductive form of PANI. Green conductive E form can be synthesized easily by electrochemical polymerization of aniline in acidic medium [51]. Electrochemical polymerization is initiated with formation of cation-radicals by monomer oxidation at the anode [52]. The green conductive E form of PANI was obtained with cyclic voltammetry in acidic medium. Cycle number is an important step for the electro-polymerization process. Depending on the cycle number, the film thickness change as was known. In order to investigate the influence of electropolymerization cycle number or the polymer thickness, PANI modification was carried out for 2, 5, 8 and 10 cycles. $[Fe(CN)_6]^{4-/3-}$ was used as redox probe to determine the electrochemical activity of the surfaces with CV. As can be seen from Fig. 7, the highest peak

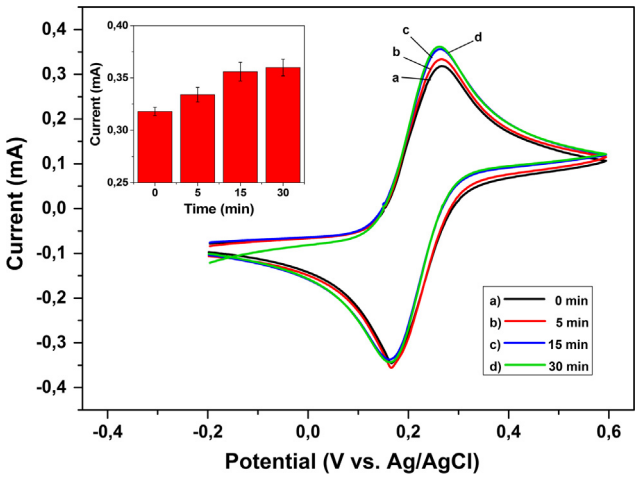

Fig. 6. Cyclic voltammograms of PANI/AuNP-PNT/PGE for different AuNP-PNT adsorption time in 0.1 M KCl solution containing 5 mM $[Fe(CN)_6]^{4-/3-}$ (−0.2/0.6 V vs. Ag/AgCl, scan rate: 0.1 V).

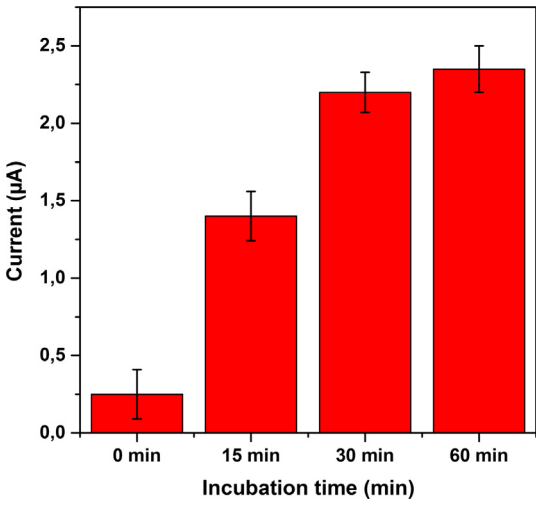

Fig. 8. The effect of the PSA incubation time on the amperometric current response of HRP/Ab2/Ag/Ab1/PANI/AuNP-PNT/PGE in 1.0 mM HQ, 0.1 mM H_2O_2 and 10 mM PBS at pH: 7.4 for 25 ng/mL PSA at an applied potential of -0.1 V (vs. Ag/AgCl).

current was recorded for the film which was produced by 5 cycles scanning. Therefore, PANI modification was done with 5 cycles in subsequent studies.

The optimization studies were completed to achieve our goal chronoamperometric studies were carried out for investigation of the PSA detection. To provide a sensitive detection the first step was to determine the optimum incubation time of PSA for binding. To accomplish the specific binding, BSA/Ab1/PANI/AuNP-PNT modified PGEs were incubated at room temperature for 15 min, 30 min, and 60 min in a solution of PSA at 25 ng/mL in PBS. Subsequently, Ab2-HRP was bounded to this surface and the steady-state current values were obtained after 150 s by the chronoamperometric method (Fig. 8). As shown in Fig. 8, it was concluded that PSA and anti-PSA bound to each other after 60 min. Thus, the binding time of PSA with anti-PSA was selected as 60 min.

3.3. Chronoamperometric PSA biosensing

Determination of PSA was performed by the chronoamperometric method using a procedure similar to the literature [53]. Electrochemical biosensor was based on a sandwich configuration where capture antibodies were immobilized to the electrode surface. Then target antigens were bound to the antibodies and HRP conjugated secondary antibodies were bound to a different epitope of the antigens. HRP reduced hydrogen peroxide in medium and this redox reaction leads a change in current that monitored by chronoamperometry [54]. If the reaction occurs in the presence of a mediator such as hydroquinone which enhances the electron transfer the overall mechanism is as follows [55].

$$H_2O_2 + HRP_{red} \rightarrow H_2O + HRP_{ox}$$

$$HRP_{ox} + HQ_{red} \rightarrow HRP_{red} + HQ_{ox}$$

$$HQ_{ox} + 2H + 2e^- \rightarrow HQ_{red}$$

$$H_2O_2 + 2e^- + 2H^+ \rightarrow 2H_2O$$

In the study, the medium used for the analysis of PSA was PBS solution containing 1 mM hydroquinone (HQ) and 1 mM H_2O_2. HQ was used as a mediator with a working potential of −0.1 V (vs. Ag/AgCl) to transfer electrons between HRP and the electrode surface. The obtained electrochemical signal of the HRP/Ab2/Ag/Ab1/PANI/AuNP-PNT/PGE electrode resulted from the redox reaction between H_2O_2 and HRP.

There was an increase in steady-state current on the chronoamperogram when increasing PSA concentration up to 100 ng/mL (Fig. 9). According to Fig. 9b, current change was linearly proportional to the concentration of PSA in a concentration range between 1 and 100 ng/mL (R^2 = 0.990). By using the following formula (Eq. (4));

$$LOD = 3\ x\ (s/m) \quad (4)$$

s: standard deviation of the blank; **m:** slope of the calibration curve.

Within the calibration range, limit of detection (LOD) was calculated as 0.68 ng/ml for biosensor. To compare the developed biosensor performance with other several electrodes in literature was given in table 1. The proposed method exhibits more linear range up to 100 ng/mL and obtained LOD value was suitable for the medical applications. Also, this method has some advantages as being disposable and cost-effectiveness according to other methods.

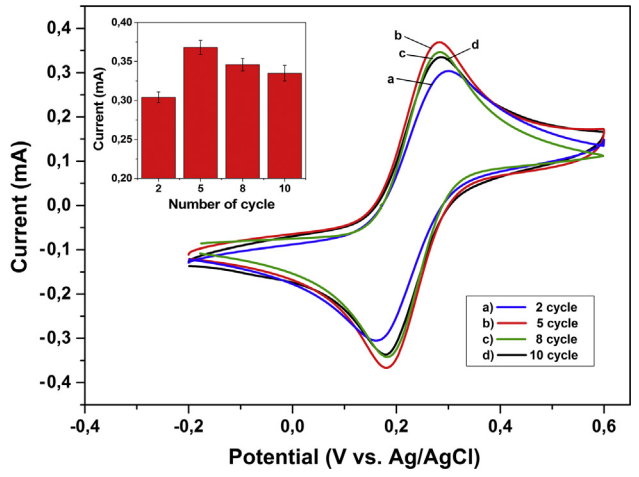

Fig. 7. The effect of applied cycle number for PANI modification of AuNP-PNT/PGE on cyclic voltammetry current in 0.1 M KCl solution containing 5 mM $[Fe(CN)_6]^{4-/3-}$ (−0.2/0.6 V vs. Ag/AgCl, scan rate: 0.1 V).

3.4. Reproducibility and stability

Reproducibility and stability of the biosensor were also investigated. To evaluate the reproducibility, five different modified elec-

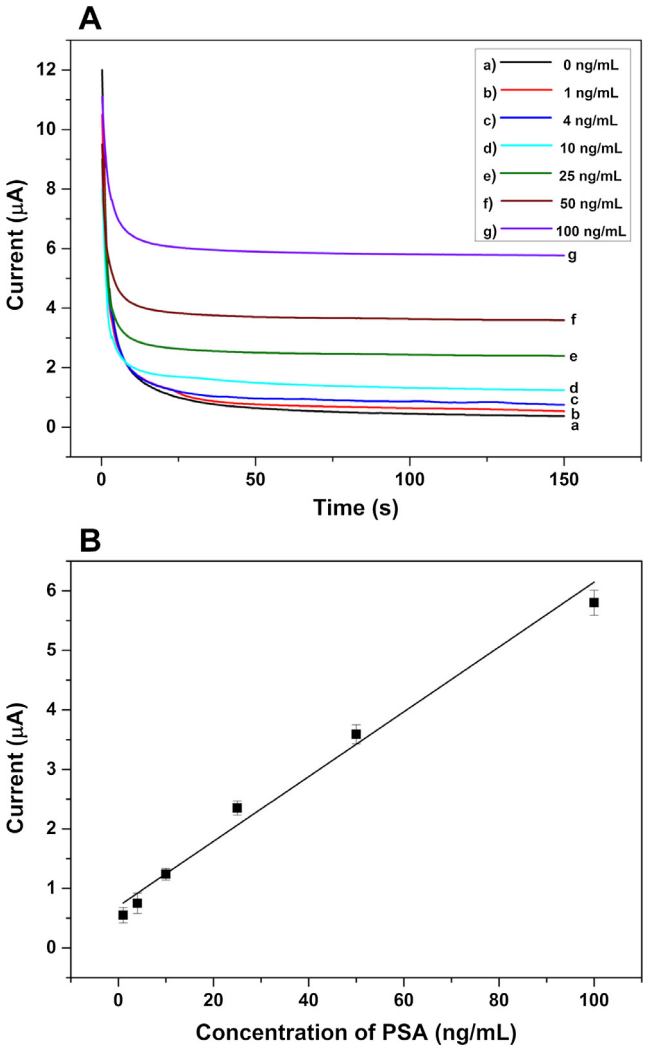

Fig. 9. (A) Chronoamperometric responses of HRP/Ab2/Ag/Ab1/PANI/AuNP-PNT/PGE in 1.0 mM HQ, 0.1 mM H_2O_2 and 10 mM PBS at pH: 7.4 for various concentrations of PSA at an applied potential of −0.1 V vs. Ag/AgCl, (scan rate: 0.1 V/s). (B) Linear calibration curve of chronoamperometric PSA detection data (1–100 ng/mL PSA).

trodes prepared in the same batch were used to measure 10 ng/mL PSA. The obtained results demonstrated that, the difference in current was not significant and the calculated relative standard deviation (RSD) was 5.6% which showed that the fabrication method was highly reproducible. For long-term stability studies, the electrodes were stored at 4 °C in a desiccator for three weeks. Every week, three electrodes were tested for 25 ng/mL PSA. After three weeks, the current response of the electrodes decreased to about 87% of the initial current value.

Table 2
Comparison of PSA levels in human serum obtained with ELISA and developed immunosensor.

Sample number	Proposed method (ng mL^{-1}) and RSD (%)	ELISA (ng mL^{-1})	Relative error (%)
1	3.42 ± 0.5 (14.7)	3.84	10.9
2	9.64 ± 1.2 (12.5)	8.64	11.6
3	22.1 ± 1.6 (7.24)	23.5	5.96
4	43.4 ± 2.9 (6.68)	45.8	5.24

95% confidence level, n = 3.

As a practical application, the developed biosensor was applied in human serum samples to detect PSA. Whole blood was collected from healthy donors and centrifuged at 3000 rpm for 5 min at room temperature to separate the serum. Different concentrations of PSA solution was added to human serum without any dilution. The results obtained by the proposed amperometric method were compared with the commercially available ELISA method.

As shown in Table 2, chronoamperometric results showed good correlation with the ELISA. The calculated maximum RSD was 14.7% and the maximum relative error was 10.9%. According to these results, it can be concluded that the biosensor was convenient for the determination of PSA in real samples.

4. Conclusion

We successfully fabricated disposable PSA biosensor based on PANI/AuNP-PNT/PGE. The electro-polymerization of aniline and the synthesis of gold nanoparticles, including peptide nanotubes, were carried out easily. It is well known that PNT and AuNP have unique electronic properties and it was observed that when composite AuNP-PNT was used to modify the PGE the electrochemical activity of the PGE surface was promoted. To the best of our knowledge, AuNP-PNT/PANI composites have never been used as a sensor application for any other analyte detection. The choronoamperometric method was carried out with the modified electrode to detect PSA with high sensitivity. The results demonstrated low detection limit (0.68 ng mL^{-1}) in a wide linear range (1–100 ng mL^{-1}) with good stability and reproducibility. The biosensor was able to measure PSA within the clinical range (1–10 ng/mL) and showed comparable results with the ELISA with good recoveries. It was shown that PSA can be detected in human serum by using cost-effective, disposable, and easily modified pencil graphite electrode. The presented strategy exhibits an effortless,

Table 1
Comparison of the proposed chronoamperometric method with some electrochemical methods.

Modification	Electrode	Method	Linear range (ng/mL)	LOD (ng/mL)	Ref.
Ferrocene-peptide	Au	SWV	5–40	0.2	[56]
Paramagnetic bead	Graphite SPE	DPV	0–10	1.7	[57]
GS-MB-CS	GCE	Amperometry	0.05–5	0.013	[58]
Phenylboronic acid	Au	Amperometry	2–15, 15–120	1.1	[59]
AuNPs	Au SPE	CV	1–10	1.0	[60]
Graphene/AuNP	GCE	CV	0–10	0.59	[61]
Platinum nanoparticles	Au	Impedance/CV	0–10	0.03	[62]
Fc-PAMAM	Au	DPV	0.01–100	0.001	[63]
MWCNTs/IL/Chit/AuPs-PAMAM	GCE	Impedance	up to 25	0.5	[64]
TB/M-CeO_2/CMC/ILs	GCE	DPV/amperometry	0.0005–50	0.00016	[65]
AuNP-peptide nanotube/PANI	PGE	Amperometry	1–100	0.68	*This study*

GS-MB-CS: graphene sheets–methylene blue–chitosan, Fc: ferrocene, MWCNTs: carbon nanotube, IL: ionic liquid, AuNPs:gold nanoparticle, PAMAM: polyamidiamine dendrimers, CMC/ILs: ionic liquids doped carboxymethyl chitosan, TB: toluidine blue, GCE: glassy carbon electrode, SPE: screen printed electrode, Au: Gold, PGE: pencil graphite electrode, SWV: Square-Wave Voltammetry, DPV: Differential Pulse Voltammetry, CV: cyclic voltammetry.

fast and economical way to determine PSA in blood serum. The procedure used to detect PSA in this study can also be applied to other biomarkers by adapting procedures that is important for point of care applications in diagnosis. In future, the modification method can be used in a miniaturized portable device for the detection of biomolecules. Also, this developed composite will be promising modification material for the electrochemical detection of various analytes.

Acknowledgement

The authors thank Hacettepe University Advanced Technologies Application and Research Center (HUNITEK) staff for their technical assistance and the Research Council of Hacettepe University for financially supporting this study (014 D02 601 004-502).

Appendix A. Supplementary material

Supplementary data associated with this article can be found, in the online version, at https://doi.org/10.1016/j.jcis.2017.09.079.

References

[1] D.L.J. Thorek, M.J. Evans, S.V. Carlsson, D. Ulmert, H. Lilja, Prostate-specific kallikrein-related peptidases and their relation to prostate cancer biology and detection, Thromb. Haemost. 110 (2013) 484–492, https://doi.org/10.1160/TH13-04-0275.
[2] H. Lilja, Biology of prostate-specific antigen, Urology 15 (2003) 27–33, https://doi.org/10.1016/S0090-4295(03)00775-1.
[3] P.S. Balk, Y.-J. Ko, G.J. Bubley, Am. Soc. Clin. Oncol. 21 (2003) 383–391.
[4] P.S. Bunting, Screening for prostate cancer with prostate-specific antigen: beware the biases, Clin. Chim. Acta 315 (2002) 71–97, https://doi.org/10.1016/S0009-8981(01)00717-3.
[5] F.J. Gruhl, K. Länge, Surface modification of an acoustic biosensor allowing the detection of low concentrations of cancer markers, Anal. Biochem. 420 (2012) 188–190, https://doi.org/10.1016/j.ab.2011.10.006.
[6] J.W. Chung, R. Bernhardt, J.C. Pyun, Additive assay of cancer marker CA 19–9 by SPR biosensor, Sens. Actuat. B 118 (2006) 28–32, https://doi.org/10.1016/j.snb.2006.04.015.
[7] Z. Altintas, I. Tothill, Biomarkers and biosensors for the early diagnosis of lung cancer, Sens. Actuat. B-Chem. 188 (2013) 988–998, https://doi.org/10.1016/j.snb.2013.07.078.
[8] Z. Onur, M. Kemal, A novel, ultra sensible biosensor built by layer-by-layer covalent attachment of a receptor for diagnosis of tumor growth, Anal. Chim. Acta 706 (2011) 343–348, https://doi.org/10.1016/j.aca.2011.08.044.
[9] M.A.M. Azmi, Z. Tehrani, R.P. Lewis, K.D. Walker, D.R. Jones, D.R. Daniels, S.H. Doak, O.J. Guy, Highly sensitive covalently functionalised integrated silicon nanowire biosensor devices for detection of cancer risk biomarker, Biosens. Bioelectron. 52 (2014) 216–224.
[10] S.A. Soper, K. Brown, A. Ellington, B. Frazier, G. Garcia-manero, V. Gau, S.I. Gutman, D.F. Hayes, B. Korte, J.L. Landers, D. Larson, F. Ligler, A. Majumdar, M. Mascini, D. Nolte, Z. Rosenzweig, J. Wang, D. Wilson, Point-of-care biosensor systems for cancer diagnostics/prognostics, Biosens. Bioelectron. 21 (2006) 1932–1942, https://doi.org/10.1016/j.bios.2006.01.006.
[11] B.V. Chikkaveeraiah, A.A. Bhirde, N.Y. Morgan, H.S. Eden, X. Chen, Electrochemical immunosensors for detection of cancer protein biomarkers, ACS Nano 6 (2012) 6546–6561, https://doi.org/10.1021/nn3023969.
[12] C. Henrik, Gorbitz, Microporous organic materials from hydrophobic dipeptides, Chem. Eur. J. 13 (2007) 1022–1031, https://doi.org/10.1002/chem.200601427.
[13] G. Chen, G. Wu, L. Wang, S. Zhang, Z. Su, Layer-by-layer assembly of single-charged ions with a rigid polyampholyte., Chem. Commun. (Camb.) (2008) 1741–1743, https://doi.org/10.1039/b801784k.
[14] A. Vakurov, C.E. Simpson, C.L. Daly, T.D. Gibson, P.A. Millner, Acetylecholinesterase-based biosensor electrodes for organophosphate pesticide detection:II. immobilization and stabilization of acetylecholinesterase, Biosens. Bioelectron. 20 (2005) 2324–2329, https://doi.org/10.1016/j.bios.2004.07.022.
[15] A. Lakshmanan, S. Zhang, C.A.E. Hauser, Short self-assembling peptides as building blocks for modern nanodevices, Trends Biotechnol. 30 (2012) 155–165, https://doi.org/10.1016/j.tibtech.2011.11.001.
[16] J. Castillo-león, K.B. Andersen, W.E. Svendsen, Self – assembled peptide nanostructures for biomedical applications: advantages and challenges, Biomater. Sci. Eng.. 2011 (InTech).
[17] Y. Zhou, Patenting activity in synthesis of lipid nanotubes and peptide nanotubes, Recent Pat. Nanotechnol. 1 (2007) 21–28, https://doi.org/10.2174/187221007779814817.
[18] N. Santhanamoorthi, P. Kolandaivel, L. Adler-Abramovich, E. Gazit, S. Filipek, S. Viswanathan, A. Strzelczyk, V. Renugopalakrishnan, Diphenylalanine peptide nanotube: charge transport, band gap and its relevance to potential biomedical applications, Adv. Mater. Lett. 2 (2011) 100–105, https://doi.org/10.5185/amlett.2010.12223.
[19] L. Laureana, P.P. Pompa, G. Maruccio, A. Della Torre, S. Sabella, A.M. Tamburro, R. Cingolani, R. Rinaldi, Charge transport and intrinsic fluorescence in amyloid-like fibrils, PNAS 104 (2007) 18019–18024.
[20] N. Ashkenasy, W.S. Horne, M.R. Ghadiri, Design of self-assembling peptide nanotubes with delocalized electronic states, Small 2 (2006) 99–102, https://doi.org/10.1002/smll.200500252.
[21] J.J. Castillo, W.E. Svendsen, N. Rozlosnik, P. Escobar, F. Martinez, J. Castillo-Leon, Detection of cancer cells using a peptide nanotube–folic acid modified graphene electrode, Analyst 138 (2013) 1026–1031, https://doi.org/10.1039/c2an36121c.
[22] M. Yemini, M. Reches, J. Rishpon, E. Gazit, Novel electrochemical biosensing platform using self-assembled peptide nanotubes, Nano Lett. 5 (2005) 183–186.
[23] M. Yemini, M. Reches, E. Gazit, J. Rishpon, T. Aviv, Peptide nanotube-modified electrodes for enzyme - biosensor applications, Anal. Chem. 77 (2005) 5155–5159.
[24] E. Chan, J. Choi, M. Lee, K. Koo, Fabrication of an electrochemical immunosensor with self-assembled peptide nanotubes, Colloids Surf. A 314 (2008) 95–99, https://doi.org/10.1016/j.colsurfa.2007.04.154.
[25] X. Dai, G.G. Wildgoose, C. Salter, A. Crossley, R.G. Compton, Electroanalysis using macro-, micro-, and nanochemical architectures on electrode surfaces. Bulk surface modification of glassy carbon microspheres with gold nanoparticles and their electrical wiring using carbon nanotubes, Anal. Chem. 78 (2006) 6102–6108, https://doi.org/10.1021/ac060582o.
[26] J.M. Pingarrón, P. Yáñez-Sedeño, A. González-Cortés, Gold nanoparticle-based electrochemical biosensors, Electrochim. Acta 53 (2008) 5848–5866, https://doi.org/10.1016/j.electacta.2008.03.005.
[27] S. Guo, E. Wang, Synthesis and electrochemical applications of gold nanoparticles, Anal. Chim. Acta 598 (2007) 181–192, https://doi.org/10.1016/j.aca.2007.07.054.
[28] S. Yalç, D. Çakmak, Electrochemical synthesis of poly (pyrrole-co-o-anisidine)/chitosan composite films, J. Mol. Struct. 1135 (2017) 32–43.
[29] K.R. Reddy, K. Lee, A.I. Gopalan, Self-assembly directed synthesis of poly (ortho -toluidine) -metal (gold and palladium) composite nanospheres, J. Nanosci. Nanotechnol. 7 (2007) 3117–3125, https://doi.org/10.1166/jnn.2007.692.
[30] K.R. Reddy, H.A.N.M.O. Jeong, Y. Lee, A.V. Raghu, Synthesis of MWCNTs-core / thiophene polymer-sheath composite nanocables by a cationic surfactant-assisted chemical oxidative polymerization and their structural properties, J. Polym. Sci. Pol. Chem. 48 (2010) 1477–1484, https://doi.org/10.1002/POLA.
[31] Y. Zhang, S. Lee, K.R. Reddy, A.I. Gopalan, K. Lee, Synthesis and characterization of core-shell SiO_2 nanoparticles/poly (3-aminophenylboronic acid) composites, J. Appl. Polym. Sci. 104 (2007) 2743–2750, https://doi.org/10.1002/app.
[32] K. Raghava, K. Lee, Y. Lee, A. Iyengar, Facile synthesis of conducting polymer – metal hybrid nanocomposite by in situ chemical oxidative polymerization with negatively charged metal nanoparticles, Mater. Lett. 62 (2008) 1815–1818, https://doi.org/10.1016/j.matlet.2007.10.025.
[33] J. Yukird, T. Wongtangprasert, R. Rangkupan, O. Chailapakul, T. Pisitkun, N. Rodthongkum, Label-free immunosensor based on graphene/polyaniline nanocomposite for neutrophil gelatinase-associated lipocalin detection, Biosens. Bioelectron. 87 (2017) 249–255, https://doi.org/10.1016/j.bios.2016.08.062.
[34] H. Rao, M. Chen, H. Ge, Z. Lu, X. Liu, P. Zou, X. Wang, H. He, X. Zeng, Y. Wang, A novel electrochemical sensor based on Au@PANI composites film modified glassy carbon electrode binding molecular imprinting technique for the determination of melamine, Biosens. Bioelectron. 87 (2017) 1029–1035, https://doi.org/10.1016/j.bios.2016.09.074.
[35] P. Rattanarat, A. Suea-Ngam, N. Ruecha, W. Siangproh, C.S. Henry, M. Srisa-Art, O. Chailapakul, Graphene-polyaniline modified electrochemical droplet-based microfluidic sensor for high-throughput determination of 4-aminophenol, Anal. Chim. Acta 925 (2016) 51–60, https://doi.org/10.1016/j.aca.2016.03.010.
[36] K. Raghava, K.V. Karthik, S.B.B. Prasad, S.K. Soni, H.M. Jeong, A.V. Raghu, Enhanced photocatalytic activity of nanostructured titanium dioxide/polyaniline hybrid photocatalysts, Polyhedron 120 (2016) 169–174.
[37] K.R. Reddy, K. Lee, A.I. Gopalan, Novel electrically conductive and ferromagnetic composites of poly (aniline- co -aminonaphthalenesulfonic acid) with iron oxide nanoparticles: synthesis and characterization, J. Appl. Polym. Sci. 106 (2007) 1181–1191, https://doi.org/10.1002/app.
[38] K.R.R. Eddy, K.L. Ee, A.I.G. Opalan, A.S. Howkat, Facile synthesis of hollow spheres of sulfonated polyanilines, Polym. J. 38 (2006) 349–354, https://doi.org/10.1295/polymj.38.349.
[39] M. Hassan, K. Raghava, E. Haque, S. Nayeem, S. Ghasemi, A.I. Minett, V.G. Gomes, Hierarchical assembly of graphene/polyaniline nanostructures to synthesize free-standing supercapacitor electrode, Compos. Sci. Technol. 98 (2014) 1–8, https://doi.org/10.1016/j.compscitech.2014.04.007.
[40] S.K. Arya, A. Dey, S. Bhansali, Polyaniline protected gold nanoparticles based mediator and label free electrochemical cortisol biosensor, Biosens. Bioelectron. 28 (2011) 166–173, https://doi.org/10.1016/j.bios.2011.07.015.
[41] X. Yu, B. Munge, V. Patel, G. Jensen, A. Bhirde, J.D. Gong, N. Sang, J. Gillespie, J.S. Gutkind, F. Papadimitrakopoulos, J.F. Rusling, S.N. Kim, J. Gillespie, J.S. Gutkind, F. Papadimitrakopoulos, J.F. Rusling, Carbon nanotube amplification strategies for highly sensitive immunosensing of cancer biomarkers, J. Am. Chem. Soc. 128 (2006) 81, https://doi.org/10.1021/ja062117e.

[42] T. Andrade-Filho, F.F. Ferreira, W.A. Alves, A.R. Rocha, The effects of water molecules on the electronic and structural properties of peptide nanotubes, Phys. Chem. Chem. Phys. 15 (2013) 7555–7559, https://doi.org/10.1039/c3cp43952f.
[43] E. Arkan, R. Saber, Z. Karimi, M. Shamsipur, A novel antibody-antigen based impedimetric immunosensor for low level detection of HER2 in serum samples of breast cancer patients via modification of a gold nanoparticles decorated multiwall carbon nanotube-ionic liquid electrode, Anal. Chim. Acta 874 (2015) 66–74, https://doi.org/10.1016/j.aca.2015.03.022.
[44] E. Laviron, General expression of the linear potential sweep voltammogram in the case of diffusionless electrochemical systems, J. Electroanal. Chem. 101 (1979) 19–28.
[45] K. Huang, L. Wang, J. Li, M. Yu, Electrochemical sensing of catechol using a glassy carbon electrode modified with a composite made from silver nanoparticles, polydopamine, and graphene, Microchim. Acta 180 (2013) 751–757, https://doi.org/10.1007/s00604-013-0988-5.
[46] J. Polte, T.T. Ahner, F. Delissen, S. Sokolov, Mechanism of gold nanoparticle formation in the classical citrate synthesis method derived from coupled in situ XANES and SAXS evaluation, J. Am. Chem. Soc. 1296–1301 (2010).
[47] I. Cherny, E. Gazit, Amyloids : not only pathological agents but also ordered nanomaterials, Angew. Chem. Int. Ed. 47 (2008) 4062–4069, https://doi.org/10.1002/anie.200703133.
[48] C.H. Gorbitz, The structure of nanotubes formed by diphenylalanine, the core recognition motif of Alzheimer's b -amyloid polypeptide, Chem. Commun. (2006) 2332–2334, https://doi.org/10.1039/b603080g.
[49] J.M. Slocik, M.O. Stone, R.R. Naik, Gold nanoparticles, Small (2005) 1048–1052, https://doi.org/10.1002/smll.200500172.
[50] B. Bozdogan, T. Vural, F. Kuralay, T. Cirak, Disposable pencil graphite electrode modified with peptide nanotubes for Vitamin B 12 analysis, Appl. Surf. Sci. 303 (2014) 37–45, https://doi.org/10.1016/j.apsusc.2014.02.039.
[51] C. Dhand, N. Dwivedi, S. Mishra, Polyaniline-based biosensors, Nanobiosensors Dis. Diagn. 4 (2015) 25–46.
[52] M.M. Gvozdenovic, B.Z. Jugovic, J.S. Stevanovic, B.N. Grgur, Electrochemical synthesis of electroconducting polymers, Hemijska Industrija 68 (2014) 673–684, https://doi.org/10.2298/HEMIND131122008G.
[53] V. Ruiz-Valdepenas Montiel, A. Pellicano, S. Campuzano, R.M. Torrente-Rodriguez, AngelJulio Reviejo, M.S. Cosio, J.M. Pingarron, Electrochemical detection of peanuts at trace levels in foods using a magnetoimmunosensor for the allergenic protein Ara h 2, Sensor Actuat. B-Chem. 236 (2016) 825–833, https://doi.org/10.1016/j.snb.2016.01.123.
[54] Z. Yang, Y. Zhuo, Y. Chai, R. Yuan, Multi-label strategy and a novel array, Sci. Rep. 4 (2014) 1–7, https://doi.org/10.1038/srep04747.
[55] H. Kim, H. Kim, C. Ahn, A. Kulkarni, M. Jeon, In situ synthesis of MoS2 on a polymer based gold electrode platform and its application in electrochemical biosensing, RSC Adv. 5 (2015) 10134–10138, https://doi.org/10.1039/C4RA14839H.
[56] N. Zhao, Y. He, X. Mao, Y. Sun, X. Zhang, C.Z. Li, Y. Lin, G. Liu, Electrochemical assay of active prostate-specific antigen (PSA) using ferrocene-functionalized peptide probes, Electrochem. Commun. 12 (2010) 471–474, https://doi.org/10.1016/j.elecom.2010.01.022.
[57] A. Zani, S. Laschi, M. Mascini, G. Marrazza, A new electrochemical multiplexed assay for PSA cancer marker detection, Electroanalysis 23 (2011) 91–99, https://doi.org/10.1002/elan.201000486.
[58] K. Mao, D. Wu, Y. Li, H. Ma, Z. Ni, H. Yu, C. Luo, Q. Wei, B. Du, Label-free electrochemical immunosensor based on graphene/methylene blue nanocomposite, Anal. Biochem. 422 (2012) 22–27, https://doi.org/10.1016/j.ab.2011.12.047.
[59] S. Liu, X. Zhang, Y. Wu, Y. Tu, L. He, Prostate-specific antigen detection by using a reusable amperometric immunosensor based on reversible binding and leasing of HRP-anti-PSA from phenylboronic acid modified electrode, Clin. Chim. Acta 395 (2008) 51–56, https://doi.org/10.1016/j.cca.2008.04.031.
[60] V. Escamilla-Gómez, D. Hernández-Santos, M.B. González-García, J.M. Pingarrón-Carrazón, A. Costa-García, Simultaneous detection of free and total prostate specific antigen on a screen-printed electrochemical dual sensor, Biosens. Bioelectron. 24 (2009) 2678–2683, https://doi.org/10.1016/j.bios.2009.01.043.
[61] H. Dong, S. Kyung, H. Chang, J. Choi, 3D label-free prostate speci fi c antigen (PSA) immunosensor based on graphene – gold composites, Biosens. Bioelectron. 63 (2015) 546–551.
[62] E. Spain, S. Gilgunn, S. Sharma, K. Adamson, E. Carthy, R. O'Kennedy, R.J. Forster, Detection of prostate specific antigen based on electrocatalytic platinum nanoparticles conjugated to a recombinant scFv antibody, Biosens. Bioelectron. 77 (2016) 759–766, https://doi.org/10.1016/j.bios.2015.10.058.
[63] E. Cevik, Ozlem Bahar, M. Senel, M.F. Abasiyanik, Construction of novel electrochemical immunosensor for detection of prostate specific antigen using ferrocene-PAMAM dendrimers, Biosens. Bioelectron. 86 (2016) 1074–1079, https://doi.org/10.1016/j.bios.2016.07.064.
[64] B. Kavosi, A. Salimi, R. Hallaj, K. Amani, A highly sensitive prostate-specific antigen immunosensor based on gold nanoparticles/PAMAM dendrimer loaded on MWCNTS/chitosan/ionic liquid nanocomposite, Biosens. Bioelectron. 52 (2014) 20–28, https://doi.org/10.1016/j.bios.2013.08.012.
[65] Y. Wei, X. Li, X. Sun, H. Ma, Y. Zhang, Q. Wei, Dual-responsive electrochemical immunosensor for prostate specific antigen detection based on Au-CoS/graphene and CeO_2/ionic liquids doped with carboxymethyl chitosan complex, Biosens. Bioelectron. 94 (2017) 141–147, https://doi.org/10.1016/j.bios.2017.03.001.